NJC

Cite this: *New J. Chem.*, 2011, **35**, 1440–1448

www.rsc.org/njc

PAPER

Long-range metal–metal coupling in transition-metal 5,10,15,20-tetraferrocenylporphyrins†

Gregory T. Rohde, Jared R. Sabin, Christopher D. Barrett and Victor N. Nemykin*

Received (in Gainesville, FL, USA) 21st February 2011, Accepted 22nd March 2011
DOI: 10.1039/c1nj20145j

Redox properties of several transition-metal MTFcP complexes ($TFcP^{2-}$ = 5,10,15,20-tetraferrocenylporphyrin, M = Co^{2+}, Ni^{2+}, Cu^{2+}, and Zn^{2+}) were investigated using electrochemical (CV and DPV), spectroelectrochemical, and chemical oxidation approaches. Electrochemical experiments conducted in a low-polarity solvent using a non-coordinating electrolyte are crucial for the sequential oxidation of ferrocene substituents along with porphyrin-based single-electron oxidation and reduction processes. The first ferrocene oxidation process in all MTFcP complexes is separated by at least 140 mV from the next three ferrocene based oxidations. The second, third, and fourth redox processes in the ferrocene region are more closely spaced, with the largest separation observed in CuTFcP and CoTFcP complexes. Mixed-valence compounds were observed and characterized by spectroelectrochemical and chemical oxidation approaches. In all cases, intervalence charge transfer (IVCT) bands were detected confirming the existence of the iron-based mixed-valence $[MTFcP]^{n+}$ (n = 1–3) species and suggesting long-range metal–metal coupling in the target systems. The resulting data from the mixed-valence $[MTFcP]^{n+}$ (n = 1–3) complexes matched very closely to the metal-free poly(ferrocenyl)porphyrins previously reported and were assigned as Robin and Day Class II mixed-valence compounds. In the case of CoTFcP, the selective oxidation of a central metal was also demonstrated in the presence of the strong ligand-field anions using oxygen as an oxidant.

Introduction

Synthesis of materials with specific optoelectronic, conductivity, or mechanistic properties is of great fundamental and technological interest.[1] Redox-active organometallic (especially ferrocene-containing) compounds which exhibit strong metal–metal coupling represent an important class of metallocomplexes potentially useful in molecular electronics.[2] Poly(ferrocenyl)-containing phthalocyanines,[3] tetraazaporphyrins,[4] corroles,[5] and especially porphyrins[6–8] have gained a lot of attention because of their diverse redox chemistry and redox-driven spectroscopic versatility. In particular, formation and stability of the corresponding mixed-valence compounds raised particular interest in these systems. The mixed-valence poly(ferrocenyl)-containing macrocycles were suggested as candidates for use in molecular electronics including, among other things, multibit information storage devices as well as redox-switchable optical and fluorescent elements active in the NIR area.[6f,k,m,o,8b] From the theoretical point of view, these compounds offer an excellent platform to study short- and long-range metal–metal coupling and electron transfer, as demonstrated in a series of poly(ferrocenyl)-containing assemblies.[6h,g,m,o,9–11] The poly-(ferrocenyl)-containing porphyrins with ferrocene substituents directly connected to the porphyrin core *via meso*-carbon atoms have recently been well characterized and were found to form several mixed-valence species.[6h,g,m,o] Indeed, in the case of the metal-free 5,10,15,20-tetraferrocenylporphyrin (H_2TFcP), 5,10,15-triferrocenyl-20-phenylporphyrin (H_2Fc_3PhP), 5,10-diferrocenyl-15,20-diphenylporphyrin (*cis*-$H_2Fc_2Ph_2P$), and 5,15-diferrocenyl-10,20-diphenylporphyrin (*trans*-$H_2Fc_2Ph_2P$), each ferrocene substituent could be oxidized individually under electrochemical, spectroelectrochemical, or chemical oxidation conditions with the formation of multiple mixed-valence species. Such mixed-valence poly(ferrocenyl)-containing porphyrins were characterized using cyclic and differential pulse voltammetry, UV-Vis-NIR, MCD, and spectroelectrochemistry. In addition, the mixed-valence states of H_2TFcP were characterized using Mössbauer, XPS, and IR methods. The characteristics of the intervalence charge transfer (IVCT) bands in the near-infrared region in these mixed-valence complexes are consistent with the valence localized, Class II (Robin and Day)[12] mixed-valence behavior. At a distance

Department of Chemistry & Biochemistry, University of Minnesota Duluth, Duluth, MN 55812, USA. E-mail: vnemykin@d.umn.edu; Fax: +1 218 726 7394; Tel: +1 218 726 6729
† Electronic supplementary information (ESI) available: DPV and IVCT data deconvolution analysis for target compounds in the DCM/TFAB system. See DOI: 10.1039/c1nj20145j

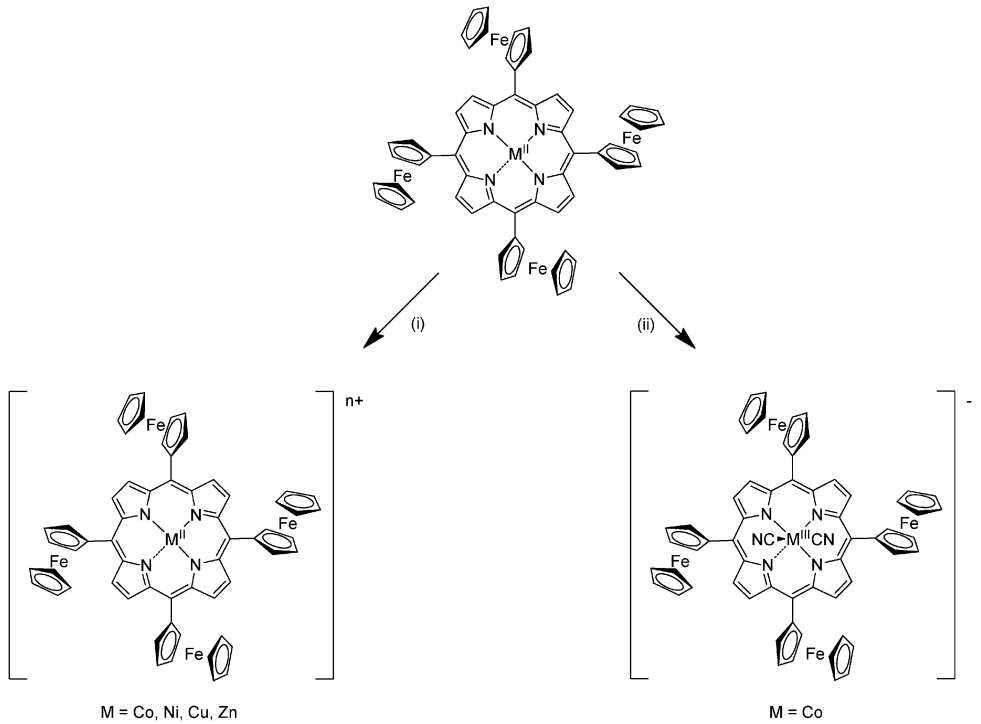

Scheme 1 *Reaction conditions*: (i) Ag^+, CCl_3CO_2H/O_2, or electrochemical oxidation; DCM. (ii) $NaCN/O_2$; DMF.

between 9.76–11.47 Å (5,10- and 5,15-porphyrin positions, respectively, determined by X-ray crystallography), the mixed-valence iron centers display relatively rare long-distance metal–metal coupling in $[H_2Fc_nPh_mP]^{x+}$ compounds.[6h,g,m,o] According to the DFT calculations and available single-crystal X-ray data, introduction of a central metal into the porphyrin cavity results in a change of the degree of non-planarity of the porphyrin core,[6l] which could potentially affect the extent of the metal–metal interactions in these systems. In addition, central metal based orbitals may influence the electron-transfer pathway. Finally, a central metal could be used to link a macrocycle to a surface when the application to molecular electronics is the final goal.[1b,d] Pursuant to the objectives mentioned above, we have investigated redox properties of the series of MTFcP (M = Co, Ni, Cu, or Zn) complexes (Scheme 1). The MTFcP mixed-valence compounds were characterized using cyclic and differential pulse voltammetry, spectroelectrochemistry, as well as UV-vis-NIR spectroscopy and compared to the well-characterized mixed-valence metal-free poly(ferrocenyl)-containing porphyrins.

Experimental section

Materials

MTFcP (M = Co, Ni, Cu, and Zn) were isolated according to the previously reported procedure.[6l] Dichloromethane (DCM) was distilled directly prior to experiments over CaH_2 and CCl_3CO_2H was distilled under reduced pressure. Tetrabutylammonium tetrakis(perfluorophenyl)borate (TFAB) was prepared according to the literature,[13] by metathesis reaction between lithium tetrakis(perfluorophenyl)borate and tetrabutylammonium bromide. All other reagents used were obtained from a commercial source and used without further purification.

Physical measurements

UV-Vis-NIR data were obtained on Jacso V-670 or Cary 17 spectrometers. MCD data were recorded using an OLIS DCM 17 CD spectropolarimeter using a permanent 1.4 T DeSa magnet. The spectra were recorded twice for each sample, once with a parallel field and again with an antiparallel field, and their intensities were expressed by molar ellipticity per $T = [\Theta]_M/\mathrm{deg\ dm^3\ mol^{-1}\ cm^{-1}\ T^{-1}}$. Electrochemical measurements were conducted using a CH electrochemical analyzer utilizing a three-electrode scheme with platinum or glassy carbon working electrodes, platinum wires as auxiliary and pseudo reference electrodes. A 0.05 M solution of dry degassed DCM and the electrolyte TFAB were used in all electrochemical experiments. Potentials were corrected using the internal standard decamethylferrocene ($Me_{10}Fc$) in all cases. Potentials were then corrected to ferrocene using appropriate oxidation potentials for $Me_{10}Fc/Me_{10}Fc^+$ *vs.* Fc/Fc^+ in the DCM/TFAB system.[13] Spectroelectrochemical data were collected in a 0.15 M solution of TFAB in DCM at the appropriate oxidation potentials using a custom made spectroelectrochemical cell. Spectroelectrochemical oxidation reversibility experiments were conducted at −0.3 V potentials.

Results and discussion

Electrochemistry of MTFcP complexes

It is well-known that polarity of the solvent and nature of the electrolyte could affect electron-transfer processes in poly(metallocenyl)-containing compounds[13,14] including

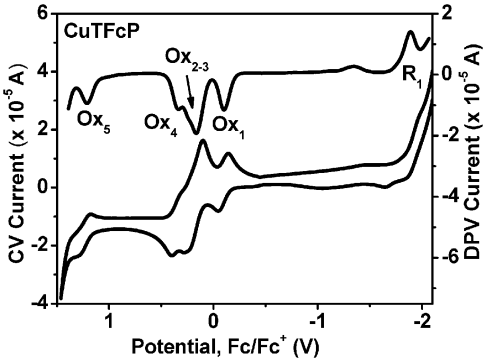

Fig. 1 Representative MTFcP DPV (upper line) and CV (lower line) for CuTFcP obtained in the DCM/TFAB system.

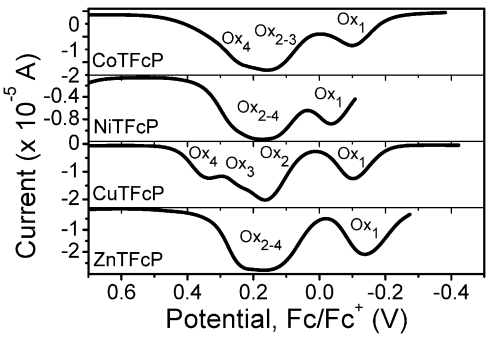

Fig. 2 DPV data on the ferrocene oxidation region of the MTFcP (M = Co, Ni, Cu and Zn) complexes in the DCM/TFAB system.

ferrocene-based oxidation waves in the H_2TFcP, H_2Fc_3PhP, *cis*-$H_2Fc_2Ph_2P$, and *trans*-$H_2Fc_2Ph_2P$ complexes.[6m,o] Thus, to minimize the interactions of the solvent and electrolyte with the redox active complex, the non-coordinating electrolyte, TFAB, and a low-polarity solvent DCM were used in this work.[13] In agreement with the previous studies on ferrocene-containing porphyrins,[6m,o] experimentally observed redox processes of MTFcP complexes (Fig. 1 and 2, Table 1; ESI†, Fig. S1) can be separated into three distinctive regions: (i) the four single-electron ferrocene-centered oxidations located between −0.1 and +0.35 V; (ii) porphyrin core/central metal single electron oxidation processes experimentally observed at potentials higher than +0.5 V; (iii) porphyrin core single electron reduction waves observed at potentials more negative than −1 V.

Based on spectroelectrochemical and chemical oxidation data presented below as well as previously discussed redox behavior of ferrocene-containing porphyrins, the first four oxidation processes (labeled as Ox1–Ox4) observed in MTFcP complexes were assigned to sequential oxidations of ferrocene substituents. Similar to H_2TFcP,[6m] the oxidation of the first ferrocene group in MTFcP complexes was always observed at a negative potential relative to ferrocene (Fig. 2, Table 1). The separation between the first and second ferrocene-centered oxidation waves of the MTFcP is quite large and ranges between 140 and 240 mV, which allows for the generation and investigation of the mixed-valence compounds of the general formula $[MTFcP]^+$. The second through fourth ferrocene-centered oxidation waves of the MTFcP are less

Table 1 Summary of the redox potentials for MTFcP complexes in the DCM/TFAB system[a]

	Ox6	Ox5	Ox4	Ox3	Ox2	Ox1	Red1	Red2
H_2TFcP[6m]		1.25	0.34	0.24	0.15	−0.07	−1.78	−2.06
CoTFcP			0.29	0.17	0.12	−0.09	−1.59(M)	−2.01
NiTFcP	1.22	0.78(M)	0.26	0.18	0.09	−0.05	−1.94	
CuTFcP		1.21	0.33	0.20	0.14	−0.10	−1.89	
ZnTFcP		1.09	0.25	0.17	0.09	−0.14	−2.03	

[a] Ox = oxidation, Red = reduction. Oxidations 1–4 are assigned to the ferrocenyl-groups and were determined by deconvolution of the DPV data with four equivalent Gaussian curves, oxidation processes 5 and 6 as well as reduction processes 1 and 2 are assigned to the porphyrin ring unless denoted (M) in which case the process is assigned to the central metal located in the porphyrin cavity. All potentials are referenced to the Fc/Fc^+ couple.

separated from each other and thus in all cases studied, DPV data were fit using Gaussian peaks in order to accurately determine respective oxidation potentials (ESI†, Fig. S1–S4). The deconvolution analysis suggests relatively small (50–90 mV) separation between the second and third ferrocene-centered oxidation potentials in all studied MTFcP. Finally, separation between third and fourth ferrocene-centered oxidation waves could be grouped into two categories. In the case of ZnTFcP and NiTFcP complexes, it is relatively small (80 mV), while it is significant for CoTFcP and CuTFcP compounds (120 and 130 mV, respectively). In all cases, the ferrocene-based oxidation processes are quasi-reversible as evident in the CV data (Fig. 1). The overall Ox1–Ox4 span for MTFcP complexes ranges between 310 (M = Ni) and 430 mV (M = Cu) and roughly follows the degree of non-planarity calculated for these compounds.[6l]

The electrochemical comproportionation constants (K_c)[15] were calculated for the all ferrocene-centered oxidation processes observed for MTFcP complexes and are presented in Table 2. As expected from the electrochemical data, the K_c for the first oxidation processes ($[MTFcP]^0 + [MTFcP]^{2+} \leftrightarrows 2[MTFcP]^+$) favor the singly oxidized species of general formula $[MTFcP]^+$, and are similar to the other ferrocenyl-containing porphyrins.[6m,o] Estimated values of K_c for the second oxidation process are significantly smaller (Table 2), suggesting potential difficulties with generation of $[MTFcP]^{2+}$ species. The relatively large values of K_c for $[CoTFcP]^{3+}$ and $[CuTFcP]^{3+}$ complexes (110 and 160, respectively) indicate that these mixed-valence complexes could be generated under spectroelectrochemical conditions. Finally, it should be noted that although estimated values of K_c could be used in characterization of the redox active species generated under spectroelectrochemical conditions, they should be treated with a great caution in discussion of the mixed-valence $[MTFcP]^{n+}$

Table 2 Summary of comproportionation constants (K_c) in MTFcP estimated using DPV electrochemical data

	$X^0 + X^{2+} \leftrightarrows 2(X^+)$	$X^{1+} + X^{3+} \leftrightarrows 2(X^{2+})$	$X^{2+} + X^{4+} \leftrightarrows 2(X^{3+})$
CoTFcP	3500	7	110
NiTFcP	230	22	23
CuTFcP	11 000	10	160
ZnTFcP	7700	22	23

compounds due to the well-documented fact that the redox potentials are highly dependent on the solvent and electrolyte.[13–16] On the other hand, spectroscopy (and specifically properties of the IVCT bands) is a better method to characterize electron coupling in the mixed-valence compounds.

Similar to the other ferrocene-containing porphyrins,[6m,o] oxidation of the porphyrin into the porphyrin cation-radical to form the $[MTFcP]^{5+/6+}$ complexes was observed at 1.22, 1.21 and 1.09 V for Ni, Cu and Zn MTFcP (Fig. 1, Table 1). An additional oxidation wave was observed for the NiTFcP complex at 0.78 V and was assigned to the Ni^{2+}/Ni^{3+} process based on redox potentials previously observed for nickel porphyrins.[17] Porphyrin ring reductions were observed for MTFcP complexes at ~ -2 V, which are similar to other porphyrin ring reductions (Table 1).[6h,g,m,o,17] In addition, an irreversible Co^{2+}/Co^{+} redox process was observed for the CoTFcP complex at -1.59 V.[17]

Spectroelectrochemistry

Spectroelectrochemistry can identify the spectrum of an *in situ* electrochemically generated species by performing bulk electrolysis at a certain potential corresponding to the specific redox process observed in cyclic and differential pulse voltammetry. The set of generated spectra can then be compared to the spectra of compounds formed by chemical oxidation to aid in the assignment of oxidation states. IVCT bands located in the NIR region are indicative of a mixed-valence ferrocenyl-containing species, and were found in a series of related mixed-valence polyferrocenyl-containing porphyrins.[6g,m,o] For instance, an IVCT band was observed for each of the following mixed-valence species: $[H_2TFcP]^{+}$, $[H_2TFcP]^{2+}$, $[H_2TFcP]^{3+}$, $[H_2Fc_3PhP]^{+}$, $[H_2Fc_3PhP]^{2+}$, and *cis*- and *trans*-$[H_2Fc_2Ph_2P]^{+}$, demonstrating that each ferrocenyl substituent could be oxidized at a different potential to form the corresponding mixed-valence state.[6m,o] In all MTFcP complexes studied, the large separation between the first and second redox waves (Fig. 1 and 2) allowed for the clean electrochemical generation of the mixed-valence $[MTFcP]^{+}$ species similar to the formation of $[H_2TFcP]^{+}$.[6m] Specifically, the rise of the IVCT bands at 840, 854, 800, and 876 nm for Co, Ni, Cu, and Zn MTFcP, respectively (Fig. 3A, 4A, 5A, and 6A), was observed and corresponded to the formation of the mixed-valence $[MTFcP]^{+}$ complexes with one Fe^{3+} and three Fe^{2+} centers. In conjunction with the formation of the $[MTFcP]^{+}$ IVCT bands, a substantial loss of the intensities of the Soret bands at 422, 430, 430, and 434 nm and the Q-bands at 664, 652, 670, and 678 nm for Co, Ni, Cu, and Zn complexes, respectively, was also observed. A band with a wavelength longer than 1600 nm was also present in the $[CuTFcP]^{+}$, $[NiTFcP]^{+}$ and $[ZnTFcP]^{+}$ spectra (Fig. 4A, 5A, and 6A) which decayed upon further oxidation. The isolation of $[MTFcP]^{2+}$ (M = Co, Cu) was not observed because the second and third ferrocene redox waves of CoTFcP and CuTFcP are closely spaced. Consistent with electrochemical observations, isolation of a second mixed-valence species, $[MTFcP]^{3+}$, was observed for M = Co and Cu because of sufficient separation between the third and fourth redox waves. Conversely, only a mixture of mixed-valence states

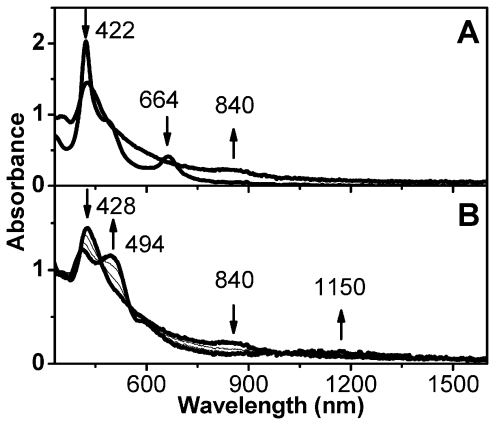

Fig. 3 Transformation of CoTFcP into $[CoTFcP]^{+}$ (A) and $[CoTFcP]^{+}$ into $[CoTFcP]^{3+}$ (B) under spectroelectrochemical conditions in the DCM/TFAB system.

was observed for MTFcP (M = Ni and Zn). The transformation from $[MTFcP]^{+}$ to $[MTFcP]^{3+}$ (M = Co, Cu; Fig. 3B and 5B) was monitored by the loss of the first IVCT band at $\sim$800 nm, the further decline of the Soret band, the loss of the low energy band around $\sim$1600 nm, and the rise of a new IVCT band at 1150 and 975 nm for Co and Cu complexes, respectively. After increasing the potential in the cell containing MTFcP (M = Ni or Zn) to the second broad redox wave, the Soret bands red shifted and decreased in intensity and new IVCT features at 975 and 928 nm for Ni and Zn (Fig. 4B and 6B, respectively) grew in the spectra. These changes and the broad nature of the IVCT band suggested the transformation of the $[MTFcP]^{+}$ to a mixture of the mixed-valence $[MTFcP]^{2+}$ and $[MTFcP]^{3+}$ species which correlates well to the small separation observed in the electrochemical experiments. The small separation between the second, third and fourth redox processes (Fig. 1 and 2, Tables 1 and 2) did not allow for the isolation of pure $[MTFcP]^{2+}$ and $[MTFcP]^{3+}$ (M = Ni and Zn) mixed-valence species, unlike what was observed for $[H_2TFcP]^{2+}$, $[H_2TFcP]^{3+}$ and $[H_2Fc_3PhP]^{2+}$.[6m,o] Finally, with the spectroelectrochemical experiments conducted at the fourth oxidation

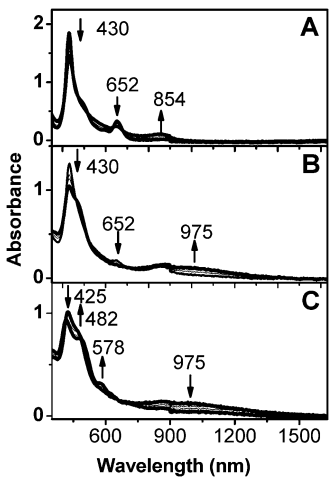

Fig. 4 Transformation of NiTFcP into $[NiTFcP]^{+}$ (A); $[NiTFcP]^{+}$ into $[NiTFcP]^{2+/3+}$ (B); and $[NiTFcP]^{2+/3+}$ into $[NiTFcP]^{4+}$ (C) under spectroelectrochemical conditions in the DCM/TFAB system.

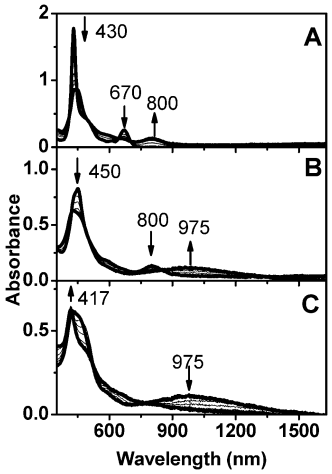

Fig. 5 Transformation of CuTFcP into $[CuTFcP]^{+}$ (A); $[CuTFcP]^{+}$ into $[CuTFcP]^{3+}$ (B); and $[CuTFcP]^{3+}$ into $[CuTFcP]^{4+}$ (C) under spectroelectrochemical conditions in the DCM/TFAB system.

potential, the disappearance of the IVCT bands in the NIR region indicated the loss of the mixed-valency of the $[MTFcP]^{4+}$ complexes (M = Ni, Cu, and Zn; Fig. 4C, 5C, and 6C). Interestingly, the solubility of the $[CoTFcP]^{4+}$ complex was not high enough for its detection. Finally, as an example of the reversibility of the redox active $[MTFcP]^{n+}$ species, electrochemical reduction of a solution of $[ZnTFcP]^{4+}$ resulted in the formation of the initial ZnTFcP complex (Fig. 6D). Notably, during reduction of $[ZnTFcP]^{4+}$, the IVCT bands reappear and diminish in the NIR as electrons are added to the ferrocenyl groups of ZnTFcP, reforming and losing the mixed-valence states as the Fe^{3+} is reduced to Fe^{2+}. The Q-band reappears at 678 nm and the Soret band returns to 434 nm (Fig. 6D).

In all cases, IVCT bands were observed for the mixed-valence $[MTFcP]^{+}$ in the NIR region similar to the IVCT bands for the previously reported $[H_2TFcP]^{+}$, $[H_2Fc_3PhP]^{+}$, and *cis*- and *trans*-$[H_2Fc_2Ph_2P]^{+}$.[6m,o] The large separation between the first and second redox waves for the MTFcP

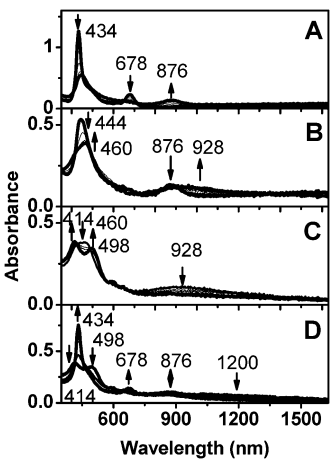

Fig. 6 Transformation of ZnTFcP into $[ZnTFcP]^{+}$ (A); $[ZnTFcP]^{+}$ into $[ZnTFcP]^{2+/3+}$ (B); $[ZnTFcP]^{2+/3+}$ into $[ZnTFcP]^{4+}$ (C); and reduction of $[ZnTFcP]^{4+}$ into ZnTFcP (D) under spectroelectrochemical conditions in the DCM/TFAB system.

allowed for the well-defined IVCT bands to be observed for the singly oxidized $[MTFcP]^{+}$ compounds. Broad IVCT bands were observed upon further oxidation of the $[MTFcP]^{+}$ and were attributed to a mixture of the $[MTFcP]^{2+}$ and $[MTFcP]^{3+}$ mixed-valence states in the cases when M = Ni and Zn because of the small separation between the second and the third oxidation potentials. The mixed-valence $[MTFcP]^{3+}$ (M = Co and Cu) complexes, and their corresponding IVCT bands were observed because of the relatively large K_c between the $[MTFcP]^{3+}$ and $[MTFcP]^{4+}$ species. The loss of the IVCT bands was observed when the $[MTFcP]^{3+}$ complexes were oxidized to the $[MTFcP]^{4+}$ state with all iron atoms in the ferric oxidation state for M = Cu, Ni, and Zn. In conjunction with the chemical oxidation data, the IVCT bands provide an estimate of the electron coupling and degree of electron delocalization and are discussed in the next section.

Chemical oxidations

In conjunction with the spectroelectrochemistry, the formation of the mixed-valence $[MTFcP]^{n+}$ complexes can be observed *in situ* by selecting appropriate chemical oxidants and following the change in the UV-Vis-NIR absorption spectrum. In agreement with electrochemical and spectroelectrochemical data, the $[MTFcP]^{+}$ mixed-valence species were able to be formed by chemical oxidation because of the large K_c between the first and second oxidation states of the ferrocene-substituted porphyrins.

Thus, the oxidation of CoTFcP by one equivalent of $AgSO_3CF_3$ produced an IVCT band at 838 nm (Fig. 7A). Also observed during the formation of $[CoTFcP]^{+}$ was a decrease in the Soret band intensity at 420 nm, a loss of the Q-band at 661 nm, and the rise of a low energy band with a wavelength longer than 2300 nm. The formation of the mixed-valence $[NiTFcP]^{+}$ by oxidation with CCl_3CO_2H and O_2[18] was noted by the decrease of the Soret band (431 nm), loss of the Q-band (654 nm) and the rise of two NIR bands at 851 nm (IVCT) and a band with a wavelength longer than 1600 nm (Fig. 8A). The chemical oxidation of CuTFcP with one equivalent of $AgSO_3CF_3$ was observed by the shift of the Soret band from 430 nm to 451 nm, the loss of the Q-band (669 nm) and the rise of two NIR bands, one around 2000 nm and the IVCT band at 803 nm signified the formation of $[CuTFcP]^{+}$ (Fig. 9A).

Finally, the oxidation of ZnTFcP with one equivalent of $AgSO_3CF_3$ also resulted in the formation of the mixed-valence $[ZnTFcP]^{+}$ (Fig. 10A) and was observed by the decline of the

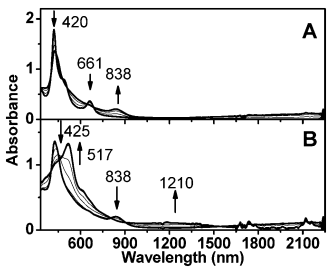

Fig. 7 Transformation of CoTFcP into $[CoTFcP]^{+}$ (A); and $[CoTFcP]^{+}$ into $[CoTFcP]^{3+}$ (B) under chemical oxidation with $AgSO_3CF_3$ as an oxidant in DCM.

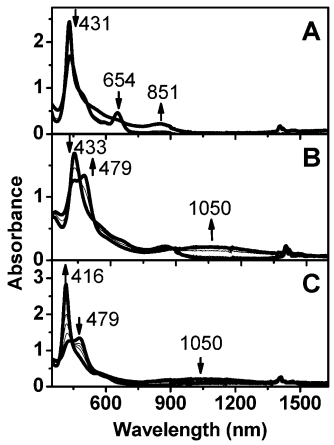

Fig. 8 Transformation of NiTFcP into $[NiTFcP]^{+}$ (A); $[NiTFcP]^{+}$ into $[NiTFcP]^{2+/3+}$ (B) and $[NiTFcP]^{2+/3+}$ into $[NiTFcP]^{4+}$ (C) under chemical oxidation with CCl_3CO_2H and O_2 as oxidants in DCM.

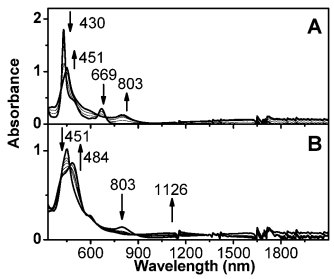

Fig. 9 Transformation of CuTFcP into $[CuTFcP]^{+}$ (A); and $[CuTFcP]^{+}$ into $[CuTFcP]^{3+}$ (B) under chemical oxidation with $AgSO_3CF_3$ as an oxidant in DCM.

Soret band (432 nm), loss of the Q-band (676 nm), the rise of the IVCT (863 nm), and the appearance of a band around 2300 nm. The formations of all $[MTFcP]^{+}$ complexes were similar to the earlier reported polyferrocenyl porphyrins[6m,o] and agreed well with spectroelectrochemical experiments discussed above.

In agreement with electrochemical and spectroelectrical data, the mixed-valence $[MTFcP]^{3+}$ (M = Co and Cu) were

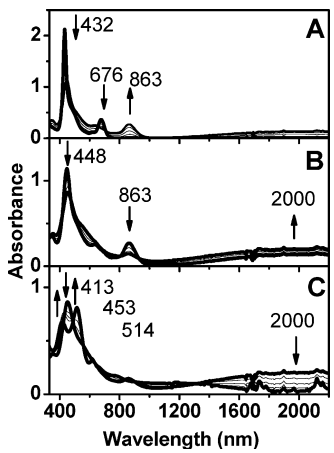

Fig. 10 Transformation of ZnTFcP into $[ZnTFcP]^{+}$ (A); $[ZnTFcP]^{+}$ into $[ZnTFcP]^{2+/3+}$ (B); and $[ZnTFcP]^{2+/3+}$ into $[ZnTFcP]^{4+}$ (C) under chemical oxidation with $AgSO_3CF_3$ as an oxidant in DCM.

able to be accessed because the K_c for these states of MTFcP (M = Co and Cu) were large enough to isolate the compounds. Oxidation with excess $AgSO_3CF_3$ resulted in the shift of the Soret band to 517 (M = Co) and 484 (M = Cu) nm, the decline of the first IVCT and low energy bands, and the rise of a broad IVCT band at 1210 (M = Co) or 1126 (M = Cu) nm (Fig. 7B and 9B) indicating the formation of $[MTFcP]^{3+}$.

The formations of mixtures of $[MTFcP]^{n+}$ (n = 1–3) were observed with further oxidation in the cases of Ni, and Zn because of the closely spaced redox potentials of second, third, and fourth redox potentials. Upon further oxidation of $[NiTFcP]^{+}$, a second broad IVCT band at 1050 nm replaced the first IVCT band along with a broadening of the Soret band and a loss of the low-energy band (Fig. 8B), which signified the formation of a mixture of $[NiTFcP]^{2+}$, and $[NiTFcP]^{3+}$ and was very similar to the transformation observed in the spectroelectrochemical experiment. After oxidation of $[ZnTFcP]^{+}$ by two equivalents of $AgSO_3CF_3$, the decline, but not loss, of the 863 nm IVCT band (indicating the presence of residual $[ZnTFcP]^{+}$), the decline of the Soret band, and the increase in intensity of the low energy band all preceded the formation of a mixture of the mixed-valence $[ZnTFcP]^{+}$, $[ZnTFcP]^{2+}$ and $[ZnTFcP]^{3+}$ (Fig. 10B). The singly oxidized species is present even after addition of two equivalents of oxidants because of the small K_c of 23 between the second and third oxidation states, resulting in the comproportionation of two $[ZnTFcP]^{2+}$ into one $[ZnTFcP]^{+}$ and one $[ZnTFcP]^{3+}$. The formation of the higher oxidized states of $[ZnTFcP]^{n+}$ was noted by a broad IVCT band around 1300 nm that became apparent after the loss of the low energy band at ~2300 nm, and the shift of the Soret band from 453 nm to two bands at 413 nm and 514 nm (Fig. 10C). Finally, in agreement with previous data, complete oxidation of the Fe^{2+} centers in NiTFcP by Cl_3COOH and O_2 to $[NiTFcP]^{4+}$ was noted by the loss of the IVCT band and interestingly a blue shift in the Soret band (Fig. 8C) to correspond to the formation of $[NiTFcP]^{4+}$.

In all cases, the $[MTFcP]^{+}$ was observed by the formation of the first IVCT band in the NIR similar to the polyferrocenyl-containing porphyrins.[6m,o] The higher oxidized states were also seen, however due to the low K_c pure species were not seen spectroscopically, except in the case of $[CoTFcP]^{3+}$ and $[CuTFcP]^{3+}$. The IVCT bands were observed at different energies with different counter ions, suggesting Robin and Day Class II (valence delocalized) mixed-valence compounds.[12,19] A more detailed examination of mixed-valence compounds involves the determination of frequency maximum (ν_{max}), the width of the band at half maximum ($\nu_{1/2}$), and the molar absorptivity (ε_{IVCT}) from the IVCT band. In the data presented here, the IVCT bands were fit with Gaussian functions to estimate these values. With these values, the electron coupling (H_{ab}, eqn (1)) and electron delocalization (α, eqn (2)) parameters were used to classify the mixed-valence compounds.[20]

$$H_{ab} = 2.05 \times 10^{-2}[(\nu_{max}\varepsilon_{max}\Delta\nu_{1/2})^{1/2}/r_{ab}] \quad (1)$$

$$\alpha^2 = 4.24 \times 10^{-4}[(\varepsilon_{max}\Delta\nu_{1/2})/(r_{ab}{}^2\nu_{max})] \quad (2)$$

Table 3 Estimated H_{ab} and α values for mixed-valence states of ferrocenyl-containing porphyrins generated under chemical- and electrochemical conditions

	ν_{max}/cm^{-1}	$\nu_{1/2}/cm^{-1}$	ε_{IVCT}	$R_{ab}{}^{d}/Å$	$H_{ab}{}^{d}$	$\alpha^2 \times 10^{3d}$
$[CoTFcP]^{+a}$	11 950	750	15 400	9.889/11.447	780/670	4.65/3.13
$[CoTFcP]^{+b}$	11 850	850	14 950	9.889/11.447	810/700	4.19/3.47
$[NiTFcP]^{+b}$	11 820	750	13 500	9.996/11.359	710/600	3.63/2.62
$[NiTFcP]^{+c}$	11 790	800	11 750	9.996/11.359	690/630	3.38/2.81
$[CuTFcP]^{+a}$	12 520	750	18 190	9.844/11.703	860/730	4.77/3.38
$[CuTFcP]^{+b}$	12 530	750	14 770	9.844/11.703	780/660	3.87/2.74
$[ZnTFcP]^{+a}$	11 575	550	18 140	9.801/11.941	710/590	3.81/2.56
$[ZnTFcP]^{+b}$	11 450	600	15 770	9.801/11.941	690/570	3.65/2.46

[a] Counter ion = $SO_3CF_3^-$. Metal centers in the *meso* position of the porphyrin ring located. [b] Counter ion = $TFAB^-$. Metal centers in the *meso* position of the porphyrin ring located. [c] Counter ion = $CCl_3CO_2^-$. Metal centers in the *meso* position of the porphyrin ring located. [d] *Syn*/*anti* conformations according to DFT calculated geometries.

Table 3 displays the parameters obtained from the IVCT band fits (ESI†, Fig. S5–S8), which are only estimates that add support to the other data collected. In all cases, the H_{ab} and α values closely match the values obtained for the previously reported polyferrocenyl porphyrins,[6m,o] and are in the range of Class II (Robin and Day) mixed-valence compounds.[12,19,20]

Oxidation of a central metal in the porphyrin core

Similar to Co(II) phthalocyanines,[21] the central Co(II) ion in the CoTFcP complex can be selectively oxidized by oxygen in the presence of axial ligands with a strong ligand field. Indeed, when the oxidation of CoTFcP with O_2 in the presence of CN^- was followed by UV-Vis-NIR spectroscopy (Fig. 11), it does not resemble the oxidation of the ferrocenyl group presented earlier (Fig. 7A). Most notably, no IVCT in the NIR region was observed during oxidation, while the Q and Soret bands red shifted from 423 to 496 nm and 675 to 727 nm, respectively, and increased in intensity (Fig. 11). The clean transformation to the putative $[Co^{III}TFcP(CN)_2]^-$ was evident by the MCD spectrum in Fig. 12. Four Faraday MCD *A*-terms dominate the MCD spectrum at 331, 381, 498, and 724 nm corresponding to transitions to doubly degenerate excited states, two of which form the most intense Soret (498), and Q (724) bands in the UV-vis spectrum. In addition, a diamagnetic ^1H NMR spectrum was also observed when CN^- was added to CoTFcP in the presence of O_2. The ^1H NMR signals for porphyrin core and ferrocene substituents in $[Co^{III}TFcP(CN)_2]^-$ were observed at 9.383 (8H; β-pyrr), 5.188 (8H; α-Cp), 4.705 (8H; β-Cp) and 3.825 (20H; CpH) and were similar to the ^1H NMR chemical shifts observed for the NiTFcP and ZnTFcP complexes.[6l] These observations demonstrate the diverse redox chemistry of the MTFcP system

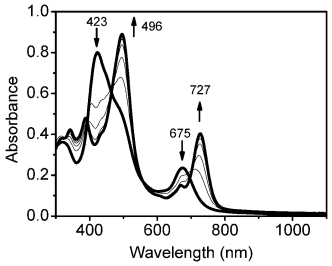

Fig. 11 Oxidation of CoTFcP by O_2 in the presence of CN^- in DMF.

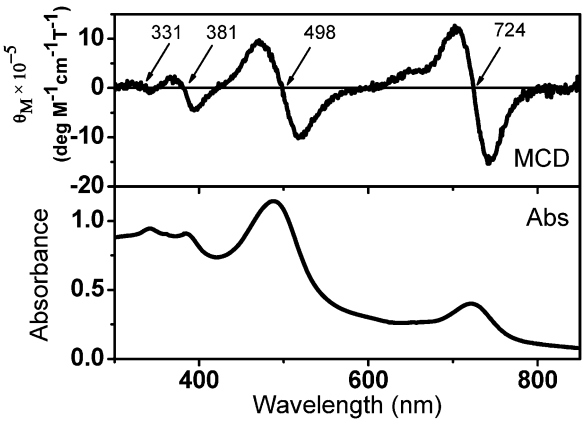

Fig. 12 MCD (top) and UV-vis spectra (bottom) of the putative $[Co^{III}TFcP(CN)_2]^-$.

to selectively oxidize the central metal or the ferrocene substituents.

Conclusions

In the presented paper, the redox properties of four transition-metal MTFcP complexes (M = Co^{2+}, Ni^{2+}, Cu^{2+}, and Zn^{2+}) were investigated using electrochemical (CV and DPV), spectroelectrochemical, and chemical oxidation approaches. Specifically, we had focused on the sequential oxidation of four ferrocene substituents connected to the porphyrin core at *meso*-carbon positions. It has been found that the electrochemical experiments conducted in a low-polarity solvent (DCM) using a non-coordinating electrolyte (TFAB) are crucial for such sequential oxidation of ferrocene substituents. The first ferrocene oxidation process in all MTFcP complexes is separated by at least 140 mV from the next three ferrocene-based oxidations. The second, third, and fourth redox processes in the ferrocene region are more closely spaced, with the largest separation observed in CuTFcP and CoTFcP complexes. When accessible, the mixed-valence compounds of general formula $[MTFcP]^{n+}$ (n = 1–3) were generated *in situ* using spectroelectrochemical and chemical oxidation approaches and characterized by the UV-vis-NIR method. In all cases, presence of the intervalence charge transfer (IVCT) bands was detected, confirming the presence

of the mixed-valence $[MTFcP]^{n+}$ (n = 1–3) species. The simultaneous presence of Fe^{2+} and Fe^{3+} centers suggests long-range metal–metal coupling in the target systems. The resulting data from the mixed-valence $[MTFcP]^{n+}$ (n = 1–3) complexes matched very closely to the previously reported[6m,o] metal-free poly(ferrocenyl)porphyrins of general formula $[H_2Fc_mPh_{4-m}P]^{n+}$ and were assigned as Robin and Day Class II mixed-valence compounds. In the case of CoTFcP, the selective oxidation of a central metal was also demonstrated in the presence of the strong ligand-field anions and oxygen as an oxidant. The resulting diamagnetic $[Co^{III}TFcP(CN)_2]^-$ complex was characterized using ^1H NMR, UV-vis, and MCD spectroscopy.

Acknowledgements

Generous support from NSF CHE-0809203 to VN, NSF GK-12 fellowship to GR and University of Minnesota Duluth Undergraduate Research Opportunity Grants to JS, and CB is greatly appreciated.

References

1 (*a*) J. R. Heath and M. A. Ratner, *Phys. Today*, 2003, **56**, 43; (*b*) J. Chen, T. Lee, J. Su, W. Wang and M. A. Reed, *Encycl. Nanosci. Nanotechnol.*, 2004, **5**, 633; (*c*) J. Weiss, *Coord. Chem. Rev.*, 2010, **254**, 2247; (*d*) *Nano and Molecular Electronics Handbook*, ed. S. E. Lyshevski, CRC Press, New York, 2007, p. 912; (*e*) H. Bayley, *Nature*, 2010, **467**, 164; (*f*) F. Giacalone and N. Martin, *Adv. Mater.*, 2010, **22**, 4220; (*g*) M. Jurow, A. E. Schuckman, J. D. Batteas and C. M. Drain, *Coord. Chem. Rev.*, 2010, **254**, 2297; (*h*) A. Chung, J. Deen, J.-S. Lee and M. Meyyappan, *Nanotechnology*, 2010, **21**, 412001; (*i*) R. V. Belosludov, A. A. Farajian, H. Baba, H. Mizuseki and Y. Kawazoe, *Jpn. J. Appl. Phys., Part 1*, 2005, **44**, 2823; (*j*) R. V. Belosludov, A. A. Farajian, Y. Kikuchi, H. Mizuseki and Y. Kawazoe, *Comput. Mater. Sci.*, 2006, **36**, 130; (*k*) S. U. Lee, R. V. Belosludov, H. Mizuseki and Y. Kawazoe, *J. Phys. Chem. C*, 2007, **111**, 15397; (*l*) S. U. Lee, R. V. Belosludov, H. Mizuseki and Y. Kawazoe, *Small*, 2008, **4**, 962.

2 (*a*) W. Kaim and G. K. Lahiri, *Angew. Chem., Int. Ed.*, 2007, **46**, 1778; (*b*) W. Kaim and B. Sarkar, *Coord. Chem. Rev.*, 2007, **251**, 584; (*c*) M. H. Chisholm and N. J. Patmore, *Acc. Chem. Res.*, 2007, **40**, 19; (*d*) B. Fabre, *Acc. Chem. Res.*, 2010, **43**, 1509; (*e*) H. Mizuseki, R. V. Belosludov, T. Uehara, S. U. Lee and Y. Kawazoe, *J. Korean Phys. Soc.*, 2008, **52**, 1197; (*f*) T. Uehara, R. V. Belosludov, A. A. Farajian, H. Mizuseki and Y. Kawazoe, *Jpn. J. Appl. Phys., Part 1*, 2006, **45**, 3768; (*g*) C. R. Arumainayagam, H.-L. Lee, R. B. Nelson, D. R. Haines and R. P. Gunawardane, *Surf. Sci. Rep.*, 2010, **65**, 1.

3 (*a*) Z. Jin, K. Nolan, C. R. McArthur, A. B. P. Lever and C. C. Leznoff, *J. Organomet. Chem.*, 1994, **468**, 205; (*b*) K.-W. Poon, Y. Yan, X. Y. Li and D. K. P. Ng, *Organometallics*, 1999, **18**, 3528; (*c*) U. Salan, A. Altindal, M. Bulut and O. Bekaroglu, *J. Porphyrins Phthalocyanines*, 2006, **10**, 1263; (*d*) V. N. Nemykin and E. A. Lukyanets, in *Handbook of Porphyrin Science*, ed. K. M. Kadish, K. M. Smith and R. Guilard, World Scientific, Singapore, 2010, vol. 3, pp. 1–323; (*e*) V. N. Nemykin and E. A. Lukyanets, *ARKIVOC*, 2010, (i), 136.

4 (*a*) V. N. Nemykin and N. Kobayashi, *Chem. Commun.*, 2001, 165; (*b*) E. A. Lukyanets and V. N. Nemykin, *J. Porphyrins Phthalocyanines*, 2010, **14**, 1.

5 (*a*) D. T. Gryko, J. Piechowska, J. S. Jaworski, M. Galezowski, M. Tasior, M. Cembor and H. Butenschoen, *New J. Chem.*, 2007, **31**, 1613; (*b*) S. Venkatraman, R. Kumar, J. Sankar, T. K. Chandrashekar, K. Sendhil, C. Vijayan, A. Kelling and M. O. Senge, *Chem.–Eur. J.*, 2004, **10**, 1423.

6 (*a*) C. Bucher, C. H. Devillers, J.-C. Moutet, G. Royal and E. Saint-Aman, *Coord. Chem. Rev.*, 2009, **253**, 21; (*b*) N. M. Loim, N. V. Abramova and V. I. Sokolov, *Mendeleev Commun.*, 1996, 46; (*c*) A. K. Burrell, W. M. Campbell, G. B. Jameson, D. L. Officer, P. D. W. Boyd, Z. Zhao, P. A. Cocks and K. C. Gordon, *Chem. Commun.*, 1999, 637; (*d*) S. J. Narayanan, S. Venkatraman, S. R. Dey, B. Sridevi, V. R. G. Anand and T. K. Chandrashekar, *Synlett*, 2000, 1834; (*e*) S. W. Rhee, Y. H. Na, Y. Do and J. Kim, *Inorg. Chim. Acta*, 2000, **309**, 49; (*f*) O. Shoji, S. Okada, A. Satake and Y. Kobuke, *J. Am. Chem. Soc.*, 2005, **127**, 2201; (*g*) O. Shoji, H. Tanaka, T. Kawai and Y. Kobuke, *J. Am. Chem. Soc.*, 2005, **127**, 8598; (*h*) A. Auger and J. C. Swarts, *Organometallics*, 2007, **26**, 102; (*i*) M. Kubo, Y. Mori, M. Otani, M. Murakami, Y. Ishibashi, M. Yasuda, K. Hosomizu, H. Miyasaka, H. Imahori and S. Nakashima, *J. Phys. Chem. A*, 2007, **111**, 5136; (*j*) V. N. Nemykin, C. D. Barrett, R. G. Hadt, R. I. Subbotin, A. Y. Maximov, E. V. Polshin and A. Y. Koposov, *Dalton Trans.*, 2007, 3378; (*k*) J. Rochford, A. D. Rooney and M. T. Pryce, *Inorg. Chem.*, 2007, **46**, 7247; (*l*) V. N. Nemykin, P. Galloni, B. Floris, C. D. Barrett, R. G. Hadt, R. I. Subbotin, A. G. Marrani, R. Zanoni and N. M. Loim, *Dalton Trans.*, 2008, 4233; (*m*) V. N. Nemykin, G. T. Rohde, C. D. Barrett, R. G. Hadt, C. Bizzarri, P. Galloni, B. Floris, I. Nowik, R. H. Herber, A. G. Marrani, R. Zanoni and N. M. Loim, *J. Am. Chem. Soc.*, 2009, **131**, 14969; (*n*) P. Galloni, B. Floris, L. de Cola, E. Cecchetto and R. M. Williams, *J. Phys. Chem. C*, 2007, **111**, 1517; (*o*) V. N. Nemykin, G. T. Rohde, C. D. Barrett, R. G. Hadt, J. R. Sabin, G. Reina, P. Galloni and B. Floris, *Inorg. Chem.*, 2010, **49**, 7497; (*p*) V. N. Nemykin and R. G. Hadt, *J. Phys. Chem. A*, 2010, **114**, 12062.

7 (*a*) A. K. Burrell, W. Campbell and D. L. Officer, *Tetrahedron Lett.*, 1997, **38**, 1249; (*b*) A. K. Burrell, W. M. Campbell, D. L. Officer, S. M. Scott, K. C. Gordon and M. R. McDonald, *J. Chem. Soc., Dalton Trans.*, 1999, 3349; (*c*) L. Jiao, B. H. Courtney, F. R. Fronczek and K. M. Smith, *Tetrahedron Lett.*, 2006, **47**, 501; (*d*) H. J. H. Wang, L. Jaquinod, M. M. Olmstead, M. G. H. Vicente, K. M. Kadish, Z. Ou and K. M. Smith, *Inorg. Chem.*, 2007, **46**, 2898; (*e*) D. T. Gryko, F. Zhao, A. A. Yasseri, K. M. Roth, D. F. Bocian, W. G. Kuhr and J. S. Lindsey, *J. Org. Chem.*, 2000, **65**, 7356; (*f*) E. S. Schmidt, T. S. Calderwood and T. C. Bruice, *Inorg. Chem.*, 1986, **25**, 3718; (*g*) K.-L. Cheng, H.-W. Li and D. K. P. Ng, *J. Organomet. Chem.*, 2004, **689**, 1593; (*h*) R. Giasson, E. J. Lee, X. Zbao and M. S. Wrighton, *J. Phys. Chem.*, 1993, **97**, 2596; (*i*) T. Muraoka, K. Kinbara and T. Aida, *Nature*, 2006, **440**, 512.

8 (*a*) G. B. Maiya, J. M. Barbe and K. M. Kadish, *Inorg. Chem.*, 1989, **28**, 2524; (*b*) P. V. Solntsev, J. R. Sabin, S. J. Dammer, N. N. Gerasimchuk and V. N. Nemykin, *Chem. Commun.*, 2010, **46**, 6581.

9 (*a*) J. S. Miller and A. J. Epstein, *Angew. Chem., Int. Ed. Engl.*, 1994, **33**, 385; (*b*) A. J. Epstein and J. S. Miller, *Synth. Met.*, 1996, **80**, 231; (*c*) S. Barlow, *Inorg. Chem.*, 2001, **40**, 7047; (*d*) S. Barlow and D. O'Hare, *Chem. Rev.*, 1997, **97**, 637; (*e*) W. Kaim and B. Sarkar, *Coord. Chem. Rev.*, 2007, **251**, 584; (*f*) *Ferrocenes: Ligands, Materials and Biomolecules*, ed. P. Stepnicka, John Wiley & Sons Ltd., Chichester, England, 2008, p. 655; (*g*) F. Ding, H. Wang, Q. Wu, T. Van Voorhis, S. Chen and J. P. Konopelski, *J. Phys. Chem. A*, 2010, **114**, 6039; (*h*) R. G. Hadt and V. N. Nemykin, *Inorg. Chem.*, 2009, **48**, 3982; (*i*) S. Santi, C. Durante, A. Donoli, A. Bisello, L. Orian, A. Ceccon, L. Crociani and F. Benetollo, *Organometallics*, 2009, **28**, 3319; (*j*) T. Y. Dong, D. N. Hendrickson, K. Iwai, M. J. Cohn, S. J. Geib, A. L. Rheingold, H. Sano, I. Motoyama and S. Nakashima, *J. Am. Chem. Soc.*, 1985, **107**, 7996; (*k*) J. A. Kramer, F. H. Herbstein and D. N. Hendrickson, *J. Am. Chem. Soc.*, 1980, **102**, 2293; (*l*) S. C. Jones, S. Barlow and D. O'Hare, *Chem.–Eur. J.*, 2005, **11**, 4473.

10 (*a*) K. Venkatasubbaiah, A. Doshi, I. Nowik, R. H. Herber, A. L. Rheingold and F. Jakle, *Chem.–Eur. J.*, 2008, **14**, 444; (*b*) K. Venkatasubbaiah, I. Nowik, R. H. Herber and F. Jaekle, *Chem. Commun.*, 2007, 2154.

11 (*a*) C. Patoux, C. Coudret, J.-P. Launay, C. Joachim and A. Gourdon, *Inorg. Chem.*, 1997, **36**, 5037; (*b*) A.-C. Ribou, J.-P. Launay, M. L. Sachtleben, H. Li and C. W. Spangler, *Inorg. Chem.*, 1996, **35**, 3735; (*c*) M. J. Cohn, M. D. Timken and D. N. Hendrickson, *J. Am. Chem. Soc.*, 1984, **106**, 6683;

(*d*) B. M. J. M. Suijkerbuijk and R. J. M. K. Gebbink, *Angew. Chem., Int. Ed.*, 2008, **47**, 7396; (*e*) P. V. Solntsev, S. V. Dudkin, J. R. Sabin and V. N. Nemykin, *Organometallics*, 2011, submitted.
12 M. B. Robin and P. Day, *Adv. Inorg. Chem. Radiochem.*, 1967, **10**, 247.
13 F. Barriere and W. E. Geiger, *J. Am. Chem. Soc.*, 2006, **128**, 3980.
14 (*a*) W. E. Geiger and N. G. Connelly, *Adv. Organomet. Chem.*, 1985, **24**, 87; (*b*) W. E. Geiger, *Organometallics*, 2011, **30**, 28; (*c*) W. E. Geiger and F. Barriere, *Acc. Chem. Res.*, 2010, **43**, 1030; (*d*) M. P. Stewart, R. Butterick III, L. G. Sneddon, Y. Matsuo and W. E. Geiger, *Inorg. Chim. Acta*, 2010, **364**, 251.
15 (*a*) D. D'Alessandro and R. Keene, *Chem. Soc. Rev.*, 2006, **35**, 424; (*b*) D. M. D'Alessandro and F. R. Keene, *Dalton Trans.*, 2004, 3950.
16 (*a*) G. E. Southard and M. D. Curtis, *Organometallics*, 2001, **20**, 508; (*b*) T. M. Figueira-Duarte, V. Lloveras, J. Vidal-Gancedo, A. Gegout, B. Delavaux-Nicot, R. Welter, J. Veciana, C. Rovira and J.-F. Nierengarten, *Chem. Commun.*, 2007, 4345; (*c*) S. Santi, L. Orian, C. Durante, E. Z. Bencze, A. Bisello, A. Donoli, A. Ceccon, F. Benetollo and L. Crociani, *Chem.–Eur. J.*, 2007, **13**, 7933; (*d*) J. Jiao, G. J. Long, L. Rebbouh, F. Grandjean, A. M. Beatty and T. P. Fehlner, *J. Am. Chem. Soc.*, 2005, **127**, 17819; (*e*) A. K. Diallo, C. Absalon, J. Ruiz and D. Astruc, *J. Am. Chem. Soc.*, 2011, **133**, 629; (*f*) Y. Ochi, M. Suzuki, T. Imaoka, M. Murata, H. Nishihara, Y. Einaga and K. Yamamoto, *J. Am. Chem. Soc.*, 2010, **132**, 5061; (*g*) D. A. Boyd, Z. Cao, Y. Song, T.-W. Wang, P. E. Fanwick, R. J. Crutchley and T. Ren, *Inorg. Chem.*, 2010, **49**, 11525; (*h*) G.-L. Xu, R. J. Crutchley, M. C. DeRosa, Q.-J. Pan, H.-X. Zhang, X. Wang and T. Ren, *J. Am. Chem. Soc.*, 2005, **127**, 13354.
17 K. M. Kadish, *Prog. Inorg. Chem.*, 1986, **34**, 435.
18 M. Castagnola, B. Floris, G. Illuminati and G. Ortaggi, *J. Organomet. Chem.*, 1973, **60**, C17.
19 (*a*) C. Creutz, *Prog. Inorg. Chem.*, 1983, **30**, 1; (*b*) N.S. Hush, *Prog. Inorg. Chem.*, 1967, **8**, 391.
20 (*a*) S. B. Piepho, E. R. Krausz and P. N. Schatz, *J. Am. Chem. Soc.*, 1978, **100**, 2996; (*b*) K. Y. Wong and P. N. Schatz, *Prog. Inorg. Chem.*, 1981, **28**, 369; (*c*) C. Creutz and H. Taube, *J. Am. Chem. Soc.*, 1969, **91**, 3988; (*d*) S. B. Piepho, *J. Am. Chem. Soc.*, 1988, **110**, 6319; (*e*) A. B. P. Lever, *Inorganic Electronic Spectroscopy*, Elsevier, Amsterdam, 2nd edn, 1984, p. 612.
21 (*a*) N. V. Kondratenko, I. N. Tretyakova, E. A. Luk'yanets, S. V. Volkov, R. K. Orlova, V. N. Nemykin and L. M. Yagupolskii, *Dyes Pigm.*, 1999, **41**, 101; (*b*) N. V. Kondratenko, V. N. Nemykin, E. A. Lukyanets, N. A. Kostromina, S. V. Volkov and L. M. Yagupolskii, *J. Porphyrins Phthalocyanines*, 1997, **1**, 341; (*c*) M. Hanack, R. Polley, S. Knecht and U. Schlick, *Inorg. Chem.*, 1995, **34**, 3621.

